Consideration of the Bimolecular Reaction Rates of $D^+(D_2O)_n$ with HCl

R. S. MacTaylor, J. J. Gilligan, D. J. Moody, and A. W. Castleman, Jr.*

Department of Chemistry, The Pennsylvania State University, University Park, Pennsylvania 16802

Received: September 3, 1998; In Final Form: January 21, 1999

The results of a detailed study of the uptake of HCl by the deuterated analogue of protonated water clusters are reported. The primary uptake of HCl is found to occur by bimolecular reaction whereupon studies at a variety of pressures indicate that no termolecular process is involved. Interestingly, varied temperature studies indicate an inverse temperature dependence on the bimolecular rate constants. The discussion is partitioned between efficiency considerations of the experimentally determined kinetics and atmospheric interpretations of HCl uptake, the latter involving comparisons to mass accommodation coefficients measured using ice films as polar stratospheric cloud mimics.

1. Introduction

One of the more active areas of research in surface chemistry involves the interaction/accommodation of a species (gas or liquid) with a surface (liquid or solid).[1−4] The common reference points for comparison of the results from various experimental endeavors is through the use of values such as mass accommodation and uptake coefficients. These terms have been defined extensively in papers concerned with unifying the results and interpretations of various research efforts in order to make significant strides toward a greater understanding of heterogeneous atmospheric chemistry.[3,4]

One of the primary objectives of the present research is to probe the microscopic details of HCl uptake by protonated water clusters both qualitatively and quantitatively. The most common method for investigating polar stratospheric cloud (PSC) relevant chemical transformations in the laboratory is the employment of thin films or surfaces of ice. The interpretations made from these results are sensitive to the fact that PSC−ice surfaces may behave somewhat differently due to the more "infinite" nature of the water−ice network. Some researchers have employed finite cluster systems in both experimental and computational studies in order to provide additional insight into PSC reactions, which are inherently tied into the "finite" size aspects of PSCs, specifically with respect to identifying the behavior at reaction sites. Water clusters, with or without the presence of an ion core, will approach mimicry of a bulk, yet finite, system as cluster size increases. Ideally, comparable results from thin film work as well as cluster studies should give a more complete and accurate picture of the chemical and physical nature of PSCs. The insight gained in the present study will be considered in terms of the results, both experimental and computational, for HCl uptake by water−ice surfaces and clusters intended to mimic PSCs.

2. Experimental Section

The fast-flow reactor employed in the present study has been described in detail previously.[5−7] It is instructive, however, to reconsider the methodology for determination of the kinetics of an ion−molecule reaction in a fast-flow reactor. Specifically, we consider the bimolecular reaction of protonated water clusters with HCl, expressed by

$$D^+(D_2O)_n + HCl \rightarrow D^+(H^+Cl^-)(D_2O)_{n-m} + mD_2O \quad (1)$$

The integrated reaction rate of eq 1 can be written

$$\ln(I/I_0) = -k[HCl]t \quad (2)$$

where t is the residence time of the ion in the reaction region of the flow tube, measured by pulsing experiments,[36] [HCl] is the concentration of HCl reactant neutral, calculated directly from the flow through a calibrated mass flow controller, and I and I_0 denote the intensities of the monitored reactant ion protonated water clusters, with and without the added reactant gas, detected by the channeltron electron multiplier (CEM). The reaction rate constant, k, is derived from the slope of the plot of the $\ln(I/I_0)$ vs [HCl] as

$$k = -\text{slope}/t \quad (3)$$

3. Results

The rate constants obtained over a range of temperatures from −140 to −120 °C and pressures from 0.25 to 0.50 Torr, are presented in Table 1. Example rate constant plots, for $D^+(D_2O)_{21}$ + HCl at −120, −130, and −140 °C, all at a pressure of 0.3 Torr, are presented in Figures 1, 2, and 3, respectively. Figure 4 shows a plot at −120 °C and a pressure of 0.5 Torr. Note, the nearly identical value in Figure 4 and the derived rate from Figure 1; a lack of pressure dependence on the rate constants was observed for all the cluster size/temperature conditions studied. The typical experimental error for these types of experiments is ±10%.[8,9] The majority of the data presented here is within these error limits; however, a few points (cluster sizes > 43) have a higher degree of uncertainty associated with them, due to low and/or fluctuating ion signal. Each rate constant value at each temperature represents the average value determined over four or more separate experiments, with an error assignment of plus or minus one standard deviation. Figure 5 depicts all the rate constants plotted against cluster size, along with the associated uncertainty for each data point.

4. Discussion

We have presented the bimolecular rate constants for the reactive incorporation of HCl into protonated water clusters D^+-

10.1021/jp983611a CCC: $18.00
Published on Web 03/17/1999

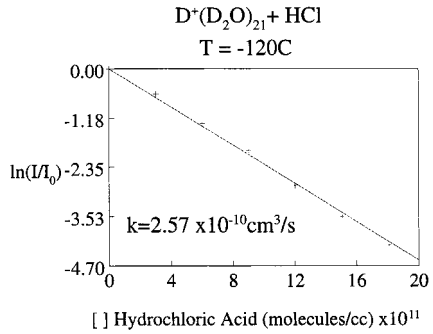

Figure 1. Example rate constant plot for $D^+(D_2O)_{21}$ + HCl at −120 °C and 0.3 Torr.

TABLE 1: $D^+(D_2O)_n$ + HCl Bimolecular Rate Constants

$D^+(D_2O)_n$ cluster size	k ($\times 10^{-10}$) cm^3/s		
	−120 °C	−130 °C	−140 °C
11	1.63 ± 0.15	2.75 ± 0.16	4.39 ± 0.40
12	1.78 ± 0.13	3.02 ± 0.18	4.75 ± 0.43
13	1.81 ± 0.15	3.47 ± 0.20	5.87 ± 0.49
14	1.96 ± 0.11	3.65 ± 0.17	5.95 ± 0.52
15	2.08 ± 0.09	3.62 ± 0.19	6.40 ± 0.59
16	2.24 ± 0.10	3.88 ± 0.23	6.21 ± 0.53
17	2.23 ± 0.09	3.65 ± 0.27	4.87 ± 0.43
18	2.44 ± 0.15	3.16 ± 0.28	5.56 ± 0.55
19	2.57 ± 0.12	2.95 ± 0.25	5.88 ± 0.53
20	2.39 ± 0.18	3.54 ± 0.23	5.65 ± 0.55
21	2.46 ± 0.16	3.74 ± 0.33	6.35 ± 0.59
22	2.32 ± 0.12	3.47 ± 0.29	5.62 ± 0.51
23	2.34 ± 0.09	3.50 ± 0.28	5.76 ± 0.52
24	2.27 ± 0.11	3.71 ± 0.30	6.06 ± 0.59
25	2.14 ± 0.18	3.58 ± 0.27	5.87 ± 0.55
26	2.19 ± 0.15	3.68 ± 0.33	6.23 ± 0.59
27	2.35 ± 0.19	3.56 ± 0.30	6.39 ± 0.61
28	2.40 ± 0.23	3.70 ± 0.33	6.52 ± 0.63
29	2.40 ± 0.17	3.69 ± 0.30	5.85 ± 0.56
30	2.43 ± 0.13	3.19 ± 0.27	5.90 ± 0.55
31	2.43 ± 0.20	3.16 ± 0.24	6.19 ± 0.60
32	2.41 ± 0.10	3.96 ± 0.31	5.76 ± 0.52
33	2.16 ± 0.16	4.08 ± 0.35	5.50 ± 0.52
34	2.19 ± 0.15	3.93 ± 0.34	5.04 ± 0.50
35	1.61 ± 0.13	3.66 ± 0.32	4.86 ± 0.49
36	1.47 ± 0.15	3.54 ± 0.27	4.76 ± 0.45
37	1.52 ± 0.11	3.42 ± 0.30	
38	1.65 ± 0.09	3.30 ± 0.31	
39	1.60 ± 0.12	3.30 ± 0.30	
40	1.65 ± 0.11	3.16 ± 0.27	
41	1.48 ± 0.09	3.01 ± 0.30	
42	1.21 ± 0.13	2.76 ± 0.26	
43	1.23 ± 0.15	3.26 ± 0.33	
44	1.47 ± 0.22	3.13 ± 0.30	
45	1.10 ± 0.20	3.30 ± 0.36	
46	0.95 ± 0.18	3.86 ± 0.39	
47	0.93 ± 0.20	3.09 ± 0.35	
48		3.42 ± 0.36	

$(D_2O)_n$ over a range of cluster sizes and temperatures. The interest and exploration of acid ionization processes is clearly evidenced in the literature.[10−31] One particularly compelling application is heterogeneous chemical conversion on PSC surfaces. Our previous work in this area, presented elsewhere,[10] provides information regarding other bimolecular channels for the uptake of a second, third, and fourth HCl into the water cluster as well as termolecular association channels for some of the higher order uptake processes. The evidence we present, however, indicates that the primary bimolecular uptake (dissolution) of HCl into the cluster is required before the termolecular channel is made accessible. We contend that the bimolecular dissolution of HCl into a cluster or onto a surface is a chemically activating first step of the molecular activation

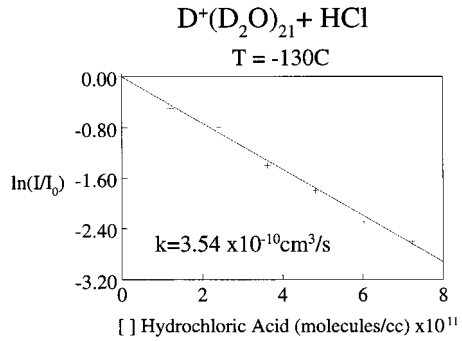

Figure 2. Example rate constant plot for $D^+(D_2O)_{21}$ + HCl at −130 °C and 0.3 Torr.

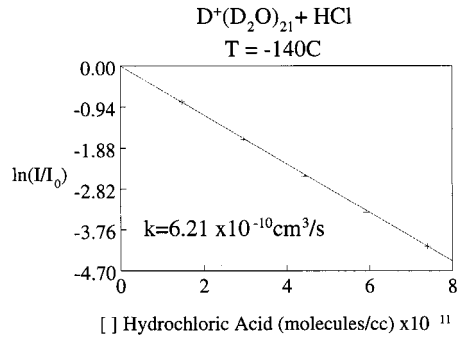

Figure 3. Example rate constant plot for $D^+(D_2O)_{21}$ + HCl at −140 °C and 0.3 Torr.

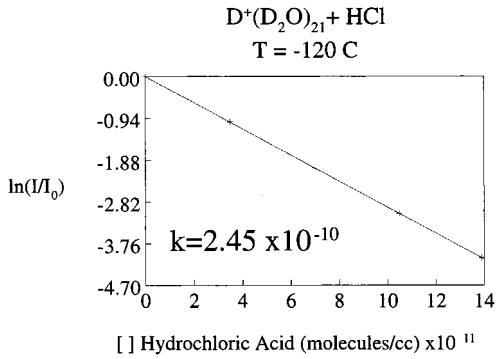

Figure 4. Example rate constant plot for $D^+(D_2O)_{21}$ + HCl at −120 °C and 0.5 Torr. Note, there is no pressure dependence on the bimolecular rate constants.

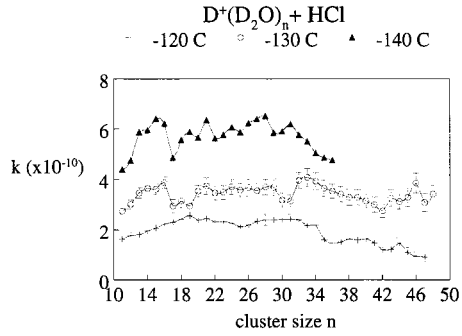

Figure 5. Rate constants (with associated uncertainty) plotted against cluster size.

by surface coordination (MASC) model[10] for heterogeneous processes involving HCl on PSCs, and it is therefore crucial to gain a deeper understanding of this process.

4.1. Reaction Efficiency. The bimolecular reaction rate constants we present in the results section provide a basis for numerous interpretations. As an initial approach, it is useful to

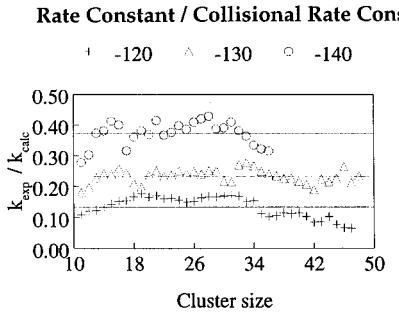

Figure 6. Ratio of experimentally determined rate constant values to the calculated collisional rate constant. The solid lines represent the average ratio at each temperature over the entire range of cluster sizes.

evaluate the efficiency of these reactions. The means by which this is accomplished is to compare the measured reaction rate to a calculated collision rate, which takes into account the average number of collisions an ion and molecule will experience in the reaction region and sets an upper bound for a measured reaction rate. Simply stated, the collision rate is the evaluated rate constant one would measure if every ion−molecule encounter resulted in a chemical reaction. There are a number of methodologies by which to determine a collision rate; we employ the Su−Chesnavich parametrized trajectory calculation.

The Su−Chesnavich approach[32,33] is a modified version of Langevin collision rate theory,[34] but takes the ion−permanent dipole interaction into account. Therefore, it is particularly applicable to ion−molecule systems such as those probed herein, where a polar neutral is involved. A thermal energy ion−polar molecule capture rate constant K_{cap} is introduced to make the corrections on the Langevin rate constant k_L.

The Langevin rate constant can be calculated as

$$k_L = 2\pi q(\alpha/\mu) \tag{4}$$

where q is the charge of the ion and μ is the reduced mass of the ion−neutral pair.

Ultimately, the corrected rate constant of an ion−molecule reaction can be calculated as $k = k_L K_{cap}$. K_{cap} is calculated utilizing the dipole moment, μ_D, and the polarizablilty, α, of the neutral reactant. The following formulas are then applied:

$$x = \mu_D/(2\alpha k_B T)^{1/2} \tag{5}$$

where k_B is the Boltzmann constant and T is temperature.

$$K_{cap}\,(\text{for } x \le 2) = (x + 0.5090)^2/10.526 + 0.972 \tag{6}$$

$$(\text{for } x \ge 2) = 0.4767x + 0.6200 \tag{7}$$

Applying this methodology for $D^+(D_2O)_n$ + HCl yields collision rates in the range of (for $n = 1-50$) 2.00×10^{-9} to 1.49×10^{-9} cm^3/s at 133 K (−140 °C), 1.95×10^{-9} to 1.46×10^{-9} cm^3/s at 143 K (−130 °C), and 1.90×10^{-9} to 1.42×10^{-9} cm^3/s at 153 K (−120 °C). Figure 6 depicts the ratio of measured rate constants divided by the calculated collision rates for the range of clusters sizes; the solid lines are the average of these values for each temperature corresponding to 0.134, 0.233, and 0.373 at −120, −130, and −140 °C, respectively.

4.2. Mass Accommodation Coefficients. These results can also be considered in the larger context of the numerous studies which have been directed toward gaining a more complete picture of the uptake and subsequent reactivity of HCl on PSC surfaces. PSC-mimic work provides information on the observed uptake of HCl by ice (water−ice and NAT) surfaces. Studies have indicated that initial coverage of a water−ice surface takes place by formation of the hexahydrate of HCl and that increased exposure to HCl results in enhanced uptake in such a ratio as to be considered HCl trihydrate coverage.[16,37,38] Our results are consistent with these observations. There is compelling experimental evidence that adsorbed HCl (DCl) dissociates ionically on ice films.[15,16,18,25] The bimolecular reactions reported here and elsewhere are consistent with ionic dissociation, whereby the enthalpy of dissolution is accommodated by "boiling off" one or more water molecules in the ion-cluster. This model is also supported by computational studies which provide thermodynamic and/or mechanistic evidence for the likelihood of ionic dissociation.[19,20,22,28] The reactivity of $HCl/ClONO_2$ is reported on water−ice surfaces and is observed to be quite efficient, which could be understood as being indicative of an ion−molecule reaction process.[11−13,39] The results of the work presented herein can be interpreted as mass accommodation coefficients which are important values necessary to treat heterogeneous processes involving HCl.

As stated above, there are numerous reports on the uptake of HCl (experimental and computational) by surfaces intended to mimic PSC behavior. One such study is provided by Hanson and Ravishankara.[13] In this experiment, HCl was allowed to react with an ice surface in a flow tube reactor attached to a chemical ionization mass spectrometer at temperatures in the range of 191 and 211 K. They found a brief period (∼3 min), displaying a constant experimental uptake coefficient of 1×10^{10} molecules/cm^3, which then decreased in value upon further exposure time. Kroes and Clary compared their computational results to experimental results and found, with certain parameters adjusted, a sticking coefficient range of 10^{-7} to 0.32, which compares reasonably well to the results of Hanson and Ravishankara in the range of 0.01 to greater than 0.3.[40] These values contrast with more recent finding by Rieley et al., who find an initial sticking coefficient of 0.95 ± 0.05 for HCl on ice in the range 80−130 K and further conclude that the HCl is exclusively ionic in nature.[25] Direct comparison of these values should be treated with caution however, as temperature is considered to be a key factor in sticking coefficients/mass accommodation coefficients.

Nathanson et al. provide numerous insights into the dynamics and kinetics at the gas−liquid interface, including experimental values and a theoretical treatment for considering the mass accommodation coefficient of HCl by water.[2] Extrapolating the values given by Nathanson et al. to colder temperatures, one soon arrives at a value close to unity. Great caution should be made in attempting to directly compare these results, because the experimental data was collected using liquid water and, obviously, the interfacial dynamics would change drastically once the liquid surface turns to ice. A trend emerges when one plots the accommodation coefficient of HCl, by the treatment described above, over a wide range of temperatures, and the result is seen in Figure 7. One immediate observation is that the mass accommodation coefficients show an inverse temperature dependence as do the bimolecular rate constants we have measured for this system. More recent insight into this phenomenon involving the heterogeneous uptake of HCl by sulfuric acid solutions clearly demonstrates the *measured* increased mass accommodation coefficient at lower temperatures.[41] The extrapolation of limited data for pure water indicates a mass accommodation coefficient of unity in the range of 140 K (Figure 7); however, it is the trend, not the specific value, which is illustrative of our point. The actual temperature at

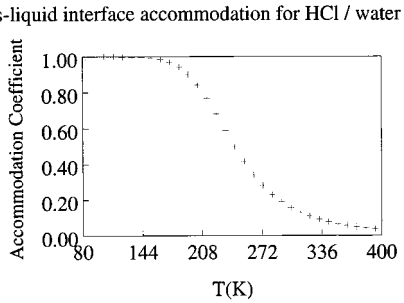

Figure 7. Extrapolation of mass accommodation coefficient treatment for the gas−liquid interface to a wide range of temperatures. Note that this is based on the limited values for the pure water system not the more recent data for sulfuric acid systems (see ref 41).

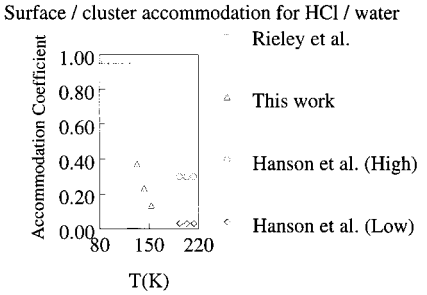

Figure 8. Experimentally determined mass accommodation coefficients at different temperatures, as described in the text.

which the mass accommodation coefficient approaches unity is probably closer to 240 K as indicated by the more extensive study involving sulfuric acid systems.

Numerous studies have probed the uptake of HCl by ice, but it is clear simply by taking these few studies into consideration that there is no definite consensus as to the mechanisms or predicted quantities involving HCl incorporation onto or into an ice surface. However, when one further considers the results presented in this work, along with those presented in our previous study,[10] one can gain some valuable insight. First of all, the initial interaction we are studying is the primary encounter and uptake of an HCl molecule by a protonated water cluster. If one considers the ratio of the experimentally determined rate constant to the calculated collision rate as a quantity depicting initial uptake of HCl, then some new thoughts emerge. The highest temperature for which the bimolecular uptake of HCl (limited by cluster size distribution) is reported is ∼150 K. The average ratio/mass accommodation coefficient at this temperature is 0.134. As the temperature is lowered, the value is 0.233 at ∼140 K, and at our lowest temperature, the value is 0.373 at ∼130 K. These data uptake versus temperature plotted in Figure 8 show a remarkable similarity to the HCl−liquid uptake data in Figure 7. These preliminary comparisons are intriguing and may eventually develop into tools for developing a greater understanding of these systems. The congruous nature between the inverse temperature dependence on our measured bimolecular rate constants and the surface studies data involving mass accommodation coefficients provides perspective on these results.

5. Conclusions

The data presented herein attempt to build the foundation necessary for the development of new treatments for heterogeneous processes involving the uptake of HCl. Perhaps some simple modifications to the gas−liquid interface models can facilitate these advancements. Clearly, more results over a greater range of temperatures and cluster sizes will aid in the analysis of this field of inquiry from a protonated water cluster aspect. Furthermore, treatment of the surface data utilizing the results from cluster studies does appear to yield some thought provoking insight into the mechanisms of HCl uptake by PSCs.

Acknowledgment. Financial support by the U.S. National Science Foundation, Atmospheric Sciences Division, Grant ATM-9711970, is gratefully acknowledged.

References and Notes

(1) Davidovits, P.; Hu, J. H.; Worsnop, D. R.; Zahniser, M. S.; Kolb, C. E. *Faraday Discuss.* **1995**, *100*, 65.
(2) Nathanson, G. M.; Davidovits, P.; Worsnop, D. R.; Kolb, C. E. *J. Phys. Chem.* **1996**, *100*, 13007.
(3) Tabazadeh, A.; Turco, R. P. *J. Geophys. Res.* **1993**, *98*, 12727.
(4) McCoustra, M. R. S.; Horn, A. B. *Chem. Soc. Rev.* **1994**, *23*, 195.
(5) Castleman, A. W., Jr.; Weil, K. G.; Sigsworth, S. W.; Leuchtner, R. E.; Keesee, R. G. *J. Chem. Phys.* **1987**, *86*, 3829.
(6) Upschulte, B. L.; Shul, R. J.; Passarella, R.; Keesee R. G.; Castleman, A. W., Jr. *Int. J. Mass. Spectrom. Ion Processes* **1987**, *75*, 27.
(7) Yang, X.; Zhang, X.; Castleman, A. W., Jr. *Int. J. Mass. Spectrom. Ion Processes* **1991**, *109*, 339.
(8) Fehsenfeld, F. C.; Schmeltekopf, A. L.; Goldan, P. D.; Schiff, H. I.; Ferguson, E. E. *J. Chem. Phys.* **1966**, *44*, 4087.
(9) Ferguson, E. E.; Fehsenfeld, F. C.; Schmeltekopf, A. L. *Adv. At. Mol. Phys.* **1969**, *5*, 1.
(10) MacTaylor, R. S.; Gilligan, J. J.; Moody, D. J., Castleman, A. W., Jr. *J. Phys. Chem.*, submitted.
(11) Abbatt, J. P. D.; Molina, M. J. *Geophys. Res. Lett.* **1992**, *19*, 461.
(12) Hanson, D. R.; Ravishankara, A. R. *J. Phys. Chem.* **1992**, *96*, 2682.
(13) Hanson, D. R.; Ravishankara, A. R. *J. Phys. Chem.* **1994**, *98*, 5728.
(14) Abbatt, J. P. D.; Beyer, K. D.; Fucaloro, A. F.; McMahon, J. R.; Wooldridge, P. J.; Zhang, R.; Molina, M. J. *J. Geophys. Res.* **1992**, *97*, 15819.
(15) Horn, A. B.; Chesters, M. A.; McCoustra, M. R. S.; Sodeau, J. R. *J. Chem. Soc., Faraday Trans.* **1992**, *88* (7), 1077.
(16) Graham, J. D.; Roberts, J. T. *J. Phys. Chem.* **1994**, *98*, 5974.
(17) Sodeau, J. R.; Banham, S. F.; Horn, A. B.; Koch, T. G. *J. Phys. Chem.* **1995**, *99*, 6258.
(18) Banham, S. F.; Horn, A. B.; Koch, T. G.; Sodeau, J. R. *Faraday Discuss.* **1995**, *100*, 321.
(19) Lee, C.; Sosa, C.; Planas, M. Novoa, J. J. *J. Chem. Phys.* **1996**, *104*, 7081.
(20) Gertner, B. J.; Hynes, J. T. *Science* **1996**, *271*, 1563.
(21) Ando, K.; Hynes, J. T. *J. Mol. Liq.* **1995**, *64*, 25.
(22) Ando, K.; Hynes, J. T. *J. Phys. Chem. B* **1997**, *101*, 10464.
(23) Marti, J.; Mauersberger, K.; Hanson, D. *Geophys. Res. Lett.* **1991**, *18*, 1861.
(24) Chu, L. T.; Leu, M.-T.; Keyser, L. F. *J. Phys. Chem.* **1993**, *97*, 7779.
(25) Rieley, H.; Aslin, H. D.; Haq, S. *J. Chem. Soc., Faraday Trans.* **1995**, *91* (15), 2349.
(26) Koch, T. G.; Banham, S. F.; Sodeau, J. R.; Horn, A. B.; McCoustra, M. R. S.; Chesters, M. A. *J. Geophys. Res.* **1997**, *102*, 1513.
(27) Schindler, T.; Berg, C. B.; Niedner-Schatteburg, G.; Bondybey, V. E. *Chem. Phys. Lett.* **1994**, *229*, 57.
(28) Buesnel, R.; Hillier, I. H.; Masters, A. J. *Chem. Phys. Lett.* **1995**, *247*, 391.
(29) Robertson, S. H.; Clary, D. C. *Faraday Discuss.* **1995**, *100*, 309.
(30) Estrin, D. A.; Kohanoff, J.; Laria, D. H.; Weht, R. O. *Chem. Phys. Lett.* **1997**, *280*, 280.
(31) Laasonen, K. E.; Klein, M. L. *J. Phys. Chem. A* **1997**, *101*, 98.
(32) Su, T.; Chesnavich, W. J. *J. Chem. Phys.* **1982**, *76*, 5183.
(33) Su, T.; Chesnavich, W. J. *J. Chem. Phys.* **1988**, *89*, 5355.
(34) Gioumousis, G.; Stevenson, D. P. *J. Chem. Phys.* **1958**, *29*, 294.
(35) Shi, Z.; Ford, J. V.; Wei, S.; Castleman, A. W., Jr. *J. Chem. Phys.* **1993**, *99*, 8009.
(36) Castleman, A. W., Jr.; Weil, K. G.; Sigsworth, S. W.; Leuchtner, R. E.; Keesee, R. G. *J. Chem. Phys.* **1987**, *86*, 3829.
(37) Koehler, B. G.; McNeill, L. S.; Middlebrook, A. M.; Tolbert, M. A. *J. Geophys. Res.* **1993**, *98*, 10563.
(38) Foster, K. L.; Tolbert, M. A.; George, S. M. *J. Phys. Chem. A* **1997**, *101*, 4979.
(39) Tolbert, M. A.; Rossi, M. J.; Malhotra, R.; Golden, D. M. *Science* **1987**, *238*, 1258.
(40) Kroes, G.-J.; Clary, D. C. *Geophys. Res. Lett.* **1992**, *19*, 1355.
(41) Robinson, G. N.; Worsnop, D. R.; Jayne, J. T.; Kolb, C. E.; Swartz, E.; Davidovits, P. *J. Geophys. Res.* **1998**, *103*, 25371.